Degenerate layer at ZnO/sapphire interface

2009 J. Phys. D: Appl. Phys. 42 195403

(http://iopscience.iop.org/0022-3727/42/19/195403)

J. Phys. D: Appl. Phys. **42** (2009) 195403 (5pp) doi:10.1088/0022-3727/42/19/195403

Degenerate layer at ZnO/sapphire interface

L Li[1,2], C X Shan[1,4], S P Wang[1,2], B H Li[1], J Y Zhang[1], B Yao[1], D Z Shen[1], X W Fan[1] and Y M Lu[3]

[1] Key Lab of Excited State Processes, Changchun Institute of Optics, Fine Mechanics and Physics, Chinese Academy of Sciences, Changchun, 130033, People's Republic of China
[2] Graduate School of The Chinese Academy of Sciences, Beijing, 100049, People's Republic of China
[3] College of Materials Science and Engineering, Shenzhen University, Shenzhen, 518060, People's Republic of China

E-mail: phycxshan@yahoo.com.cn

Received 19 June 2009, in final form 4 August 2009
Published 14 September 2009
Online at stacks.iop.org/JPhysD/42/195403

Abstract
Zinc oxide (ZnO) films have been prepared on sapphire substrates by molecular beam epitaxy. It is found that the electron concentration of the films decreases, while the mobility increases with increasing the film thickness. Temperature-dependent Hall measurement reveals the existence of a degenerate layer at the ZnO/sapphire interface, which will increase the electron concentration and decrease the mobility in the ZnO film. By using a two-layer conduction model, the electron concentration and mobility of the film excluding the influence of the degenerate layer have been determined. A fitting to the corrected electron concentration of the ZnO film yields an activation energy of about 31 meV for the residual donors.

(Some figures in this article are in colour only in the electronic version)

1. Introduction

Due to their large binding energy (60 meV), excitons in ZnO are thermally stable at room or even higher temperature, which is a significant advantage in light emitting devices and laser diodes [1, 2]. However, one of the major obstacles hindering such applications lies in the huge difficulty in realizing p-type ZnO. To make extrinsic p-type doping of ZnO films possible, an important prerequisite is that high-quality undoped ZnO films with low residual electron concentration and high electron mobility will be obtained. Because of the large lattice mismatch (18%) and thermal mismatch between ZnO and sapphire, the general substrate employed for the growth of ZnO films, a thin, highly dislocated region will be generated at the layer/substrate interface to relieve the strain [3]. The interfacial layer, which will be called a degenerate layer in the following text, has a huge influence on the carrier transportation of the films, and thus may cause a significant discrepancy between the carrier concentration and mobility values measured by Hall measurement and the actual values. Therefore, clarifying the effect of the degenerate layer on the carrier transportation in ZnO films is of great significance. The electrical, structural properties of such a degenerate layer in GaN films have been studied in great detail [4–6, 8]. However, only one report demonstrating the effect of the degenerate layer on the Hall data of ZnO films can be found to the best of our knowledge [7], where the substrate employed is glass, which is an uncommon substrate for ZnO films. Therefore, it will be more significant to study the effect of the degenerate layer on the residual electron concentration and mobility of ZnO films grown on sapphire substrates.

In this paper, the interface conductance of ZnO films grown on sapphire has been investigated by the temperature-dependent Hall measurement, and the electron concentration and mobility in the ZnO film have been corrected in terms of a two-layer conduction model considering the existence of a degenerate layer at the interface. A fitting to the corrected electron concentration gives an activation energy of about 31 meV for the residual donor-related defects in ZnO.

2. Experiments

The ZnO thin films studied in this paper were grown on *c*-plane sapphire (Al_2O_3) substrates using a plasma-assisted molecular beam epitaxy (MBE) technique. To obtain a clean fresh

[4] Author to whom any correspondence should be addressed.

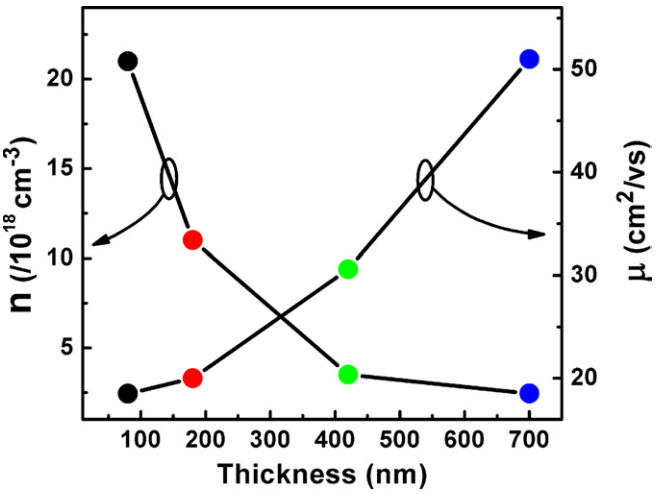

Figure 1. The dependence of the electron concentration and mobility in the ZnO films on their thickness.

surface, the substrates were treated by acetone and ethanol in an ultrasonic bath, then chemically etched in H_2SO_4 : H_3PO_4 = 3 : 1 at 160 °C for 15 min and then rinsed with deionized water (18.2 MΩ cm^{-1}) and blown dry using nitrogen gas. They were then thermally pre-treated at 750 °C for 30 min before being loaded into the growth chamber, which was expected to remove the surface contaminants of the Al_2O_3 substrates. Metallic zinc (99.9999%) and oxygen gas (99.9999%) were employed as the precursors. A Knudsen effusion cell was used to evaporate elemental zinc, and the O_2 was activated by an Oxford Applied Research Model HD25 radio-frequency (13.56 MHz) atomic source operating at 300 W. The substrate temperature was kept at 800 °C, the O_2 flow at 0.80 sccm (sccm denotes standard cubic centimetre per minute) and the pressure in the MBE chamber was maintained at 1.5×10^{-5} mbar during the growth process. By keeping the other parameters constant except the growth duration, four ZnO films with different thicknesses were prepared. The surface morphology of the films was investigated by a field-emission scanning electron microscope (SEM, Hatachi S4800). The structural properties of the ZnO films were characterized in a Rigaku D/max-RA x-ray diffractometer (XRD) using Cu Kα line (Kα1 = 1.5405 Å, Kα2 = 1.5443 Å) as the irradiation source. The carrier concentration and mobility of the films were studied by Hall measurement (LakeShore 7707) under the Van der Pauw configuration. The temperature-dependent Hall measurement was conducted over the temperature range from 85 to 425 K using a continuous flow liquid-nitrogen cooling system. The Hall data were compiled employing both positive and negative currents and magnetic fields, and the results were averaged in order to compensate various electromagnetic effects.

3. Results and discussion

Figure 1 shows the variation of the electron concentration and mobility of the ZnO films with their thickness. The electron concentration of the 80 nm ZnO film is as high as 2.1×10^{19} cm^{-3}, and the concentration decreases gradually with increasing thickness of the ZnO films. In contrast, the

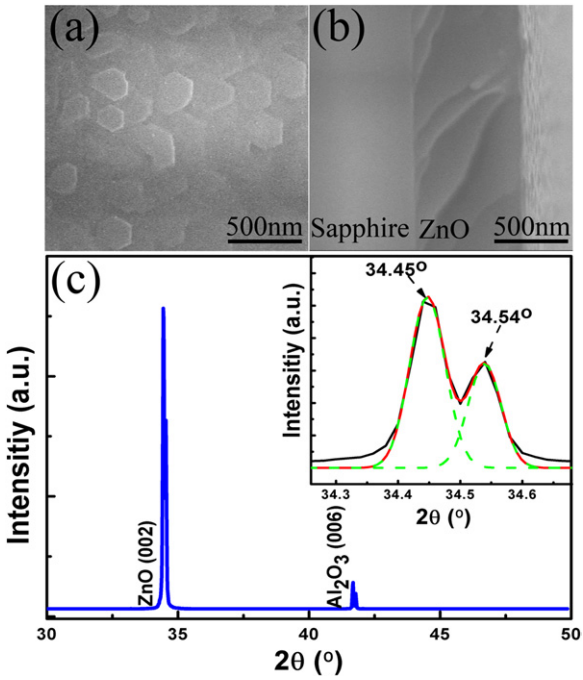

Figure 2. Plan-view (*a*) and cross-sectional (*b*) SEM images and XRD pattern (*c*) of the ZnO film with a thickness of 700 nm.

electron mobility increases with increasing thickness of the ZnO films. That is, the electron concentration and mobility are closely related to the film thickness. A similar phenomenon has also been observed in GaN [4, 8] and InN films [9, 10], and it has been considered to result from a degenerate layer at the GaN/sapphire interface in GaN films [4, 5, 8]. This degenerate layer has a relatively high defect density, thus the electron concentration in this layer is relatively high. This conductive degenerate layer will have a huge impact on the Hall measurement, leading to a significant discrepancy between the actual and the measured value. The existence of such a degenerate layer at the ZnO/sapphire interface has been demonstrated by Tampo *et al* [3].

To investigate the effect of the degenerate layer in detail, the as-grown ZnO film with a thickness of 700 nm was selected as a representative. Figures 2(*a*) and (*b*) shows the surface morphology and cross sectional image of the ZnO film. The film shows a flat surface, on which many regular hexagons can be seen. The XRD pattern of the ZnO film is shown in figure 2(*c*); besides the peak from the Al_2O_3 substrate, only the ZnO (0 0 2) diffraction peak can be observed. Note that the ZnO (0 0 2) diffraction peak consists of two satellite peaks coming from the diffraction from Cu Kα1 and Kα2 lines, as shown in the inset of figure 2(*b*), and the full width at half maximum (FWHM) of the two satellite peaks are 0.054° and 0.049°, respectively. The above results indicate that the as-grown ZnO film is crystallized in a wurtzite structure with (0 0 2) preferred orientation. The SEM image, together with the XRD pattern, reveals that the film is of acceptably high crystalline quality, which ensures that the ZnO film can serve as a solid platform for the study of the effect of the degenerate layer on the Hall measurement.

Temperature-dependent electron concentration of the ZnO film is shown in figure 3. The electron concentration

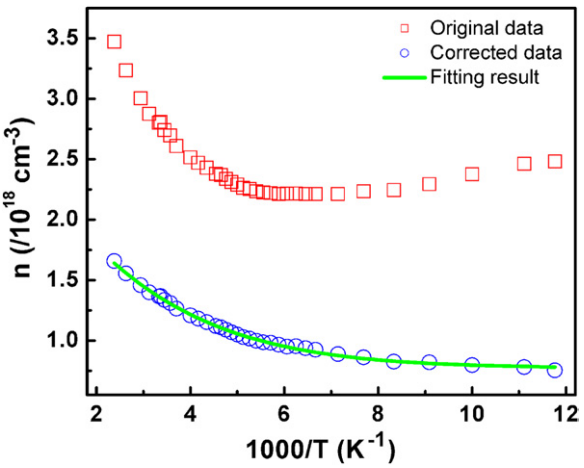

Figure 3. Temperature-dependent electron concentration obtained by the Hall measurement (squares) and the corrected bulk electron concentration data (circles), the solid curve is the fitting result to the corrected data.

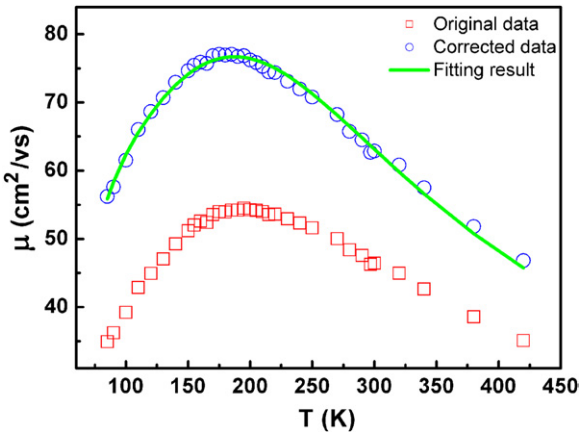

Figure 4. Electron mobility data obtained by the Hall measurement at different temperatures (squares) and the corrected bulk mobility data (circles), the solid curve shows the fitting result to the corrected data.

decreases significantly when the temperature decreases from 425 to 170 K, which is a classical deionization process of donors, then increases slightly as temperature decreases further. A similar phenomenon has been observed in GaN [4, 6] and ZnO [3], and regarded as an indication of parallel conduction of two conducting layers, which are defined as the bulk layer at the top part of the ZnO film and the degenerate layer at the ZnO/sapphire interface. The electron concentration and mobility of the bulk layer can be denoted by n_1 and μ_1, while those of the degenerate layer by n_2 and μ_2, and n_H and μ_H represent the electron concentration and mobility values obtained by the Hall measurement. In the degenerate layer, the electron concentration can be assumed to be temperature-independent. Hence, the electron concentration of the degenerate layer (n_2) can be deduced approximately by extrapolating the variation trend of the electron concentration measured by the Hall measurement with temperature approaching 0 K. Similarly, the mobility of the degenerate layer (μ_2) can be obtained using the same method. In this way, the electron concentration and mobility in the degenerate layer obtained are $n_2 = 3.05 \times 10^{18}\,\mathrm{cm}^{-3}$ and $\mu_2 = 14.5\,\mathrm{cm}^2\,\mathrm{V}^{-1}\,\mathrm{s}^{-1}$, respectively.

A two-layer conduction model developed by Look *et al* can be used to calculate the electron concentration and mobility in the bulk layer, the formulae are listed below [4]:

$$n_1 = \frac{(\mu_H n_H - \mu_2 n_2)^2}{\mu_H^2 n_H - \mu_2^2 n_2}, \tag{1}$$

$$\mu_1 = \frac{\mu_H^2 n_H - \mu_2^2 n_2}{\mu_H n_H - \mu_2 n_2}. \tag{2}$$

By inserting the measured electron concentration and mobility of the ZnO film (μ_H and n_H) and the deduced data of the degenerate layer (μ_2 and n_2) into equations (1) and (2), the corresponding electron concentration and mobility values of the bulk layer (μ_1 and n_1) can be obtained, the dependence of which on temperature is shown by scattered circles in figures 3 and 4. One can see from the figures that both the electron concentration and mobility in the bulk layer are significantly different from the corresponding values determined by the Hall measurement, which reveals that the degenerate layer does have a huge effect on the carrier concentration and mobility data of the ZnO film in the whole investigated temperature range (85–425 K). Especially for the room temperature mobility (μ_1) and electron concentration (n_1), which are often used as a figure of merit of intrinsic ZnO films, the corrected mobility excluding the effect of the degenerate layer is distinctively higher (63 versus $46\,\mathrm{cm}^2\,\mathrm{V}^{-1}\,\mathrm{s}^{-1}$), while the electron concentration is lower (1.3×10^{18} versus $2.8 \times 10^{18}\,\mathrm{cm}^{-3}$) than the data obtained by the Hall measurement (μ_H, n_H).

The relationship between the bulk electron concentration and temperature can be well fitted by using a single-donor model [11]:

$$n + N_A = \frac{N_D}{1 + n/\phi}, \tag{3}$$

where n is the electron concentration, N_A and N_D are the acceptor and donor concentration, respectively. ϕ is expressed by the following formula:

$$\phi = (g_0/g_1) N_C T^{3/2} \exp(-E_D/KT). \tag{4}$$

Here, g_0 and g_1 are the degeneracy of the unoccupied and occupied donor states, respectively, $N_C = (2(2\pi m_n^* K)^{3/2}/h^3)$ is the effective conduction-band density of states at $T = 1$ K, which can be quantified to be $8.66 \times 10^{20}\,\mathrm{m}^{-3}$ by inserting all the values of the parameters into the above equation, E_D is the activation energy of the donor, and N_D, N_A and E_D are fitting parameters. The best fitting using equation (3) to the dependence of the corrected electron concentration on temperature yields the following values: $N_D = 1.76 \times 10^{18}\,\mathrm{cm}^{-3}$, $N_A = 7.6 \times 10^{17}\,\mathrm{cm}^{-3}$ and $E_D = 31$ meV. The activation energy of the residual donor we obtained is in reasonable agreement with the reported value of 25–40 meV [12–16], which confirms the validity of our fitting.

As for the mobility data, in order to analyse the corrected data, the following five scattering channels limiting the

mobility have to be considered. The parameters involved in the mobility equations are listed below [17–19]: electron effective mass $m^* = 0.318m_0$, low-frequency dielectric constant $\varepsilon_0 = 8.12 \times (8.8542 \times 10^{-12})\,\mathrm{F\,m^{-1}}$, high-frequency dielectric constant $\varepsilon_\infty = 3.72 \times (8.8542 \times 10^{-12})\,\mathrm{F\,m^{-1}}$, piezoelectric coupling coefficient $P = 0.21$, longitudinal lattice constant $c = 5.207\,\text{Å}$, longitudinal optical phonon energy $\hbar\omega = 72\,\mathrm{meV}$, acoustic deformation potential $E_c = 15\,\mathrm{eV}$, Debye temperature $T = 837\,\mathrm{K}$ and longitudinal elastic constant $c_l = 2.47 \times 10^{11}\,\mathrm{N\,m^{-2}}$. k is Boltzman's constant, $\hbar$ is Planck's constant divided by 2π, e is the electron charge, T is the absolute temperature. The contribution from the five channels can be expressed using the following equations.

(I) Mobility caused by ionized-impurity scattering [17]:

$$\mu_{\mathrm{ii}} = \frac{128\sqrt{2\pi}\varepsilon_0^2(kT)^{3/2}}{N_\mathrm{I}e^3\sqrt{m^*}\left[\ln(1+y) - \frac{y}{1+y}\right]} = \frac{383\,797 \times 10^{18} \times T^{3/2}}{N_\mathrm{I}\left[\ln(1 + 0.3 \times 10^{-4} \times T^2) - \frac{0.3\times10^{-4}\times T^2}{1+0.3\times10^{-4}\times T^2}\right]}. \quad (5)$$

Here $y = 24\varepsilon_0 m^*(kT)/\hbar^2 e^2 n$, N_I is the ionized-impurity concentration in the ZnO film.

(II) Mobility caused by grain boundary scattering [20, 21]:

$$\mu_\mathrm{b} = \frac{el}{\pi m^*}\exp\left(-\frac{\phi_\mathrm{b}}{kT}\right) = 159 \times L \times T^{-1/2} \times \exp\left(-\frac{\phi_\mathrm{b}}{kT}\right). \quad (6)$$

Here l is the grain size, ϕ_b is the grain barrier height.

(III) Acoustical phonon deformation potential scattering [22]:

$$\mu_{\mathrm{as}} = 6.12 \times 10^6 \times T^{-3/2}. \quad (7)$$

(IV) Piezoelectric scattering [22]:

$$\mu_{\mathrm{pz}} = 4.62 \times 10^5 \times T^{-1/2}. \quad (8)$$

(V) Mobility caused by polar optical-mode scattering. Since this kind of scattering is inelastic, by solving the Boltzmann equation using Kohler's variational technique [23], the following expression can be written [24, 25]:

$$\mu_{\mathrm{pop}} = \frac{2^{9/2}\pi^{1/2}\hbar^2(kT)^{1/2}(e^{T_{\mathrm{po}}/T} - 1)\chi(T_{\mathrm{po}}/T)}{3e(kT_{\mathrm{po}})m^{*3/2}(\varepsilon_\infty^{-1} - \varepsilon_0^{-1})}, \quad (9)$$

where $T_{\mathrm{po}} = \hbar\omega/k$, $\chi(T_{\mathrm{po}}/T)$ is a slowly varying function of temperature. Because the polar optical phonon scattering plays an important role at high temperature, and the temperature is located at $84\,\mathrm{K} \leqslant T \leqslant 420\,\mathrm{K}$ in our experiment, hence, $\chi(T_{\mathrm{po}}/T) \approx 1$ [24]. By substituting the known parameters into equation (9), then

$$\mu_{\mathrm{pop}} = 1.2 \times (\mathrm{e}^{\hbar\omega/kT} - 1) \times T^{1/2}. \quad (10)$$

The total mobility can be approximated according to Matthiessen's rule:

$$\mu_{\mathrm{Total}}^{-1} = \mu_{\mathrm{ii}}^{-1} + \mu_{\mathrm{grain}}^{-1} + \mu_{\mathrm{ac}}^{-1} + \mu_{\mathrm{pe}}^{-1} + \mu_{\mathrm{pop}}^{-1}. \quad (11)$$

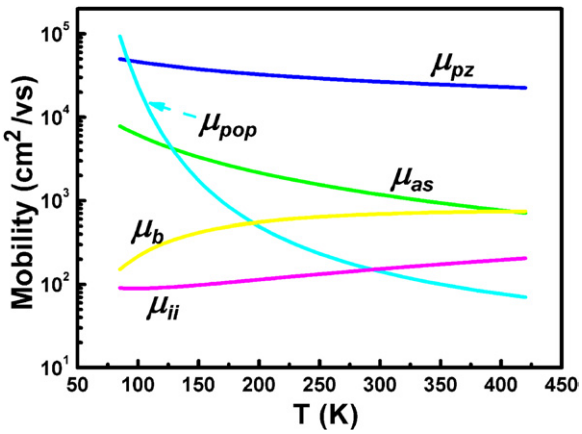

Figure 5. The mobility determined by the five scattering channels at different temperatures.

By fitting the dependence of the corrected mobility data on temperature using equation (11), as shown by the solid curve in figure 4, the grain size L and the grain barrier height ϕ obtained from the fitting are 175 nm and 22 meV, respectively. We note that the grain size obtained from the fitting is in reasonable agreement with that observed in the SEM image shown in figure 2 (around 200 nm), and the barrier height, 22 meV, is in good accord with the values reported in ZnO films grown on a sapphire substrate (about 20 meV) [26], which in turn, confirms the validity of our fitting.

By substituting the acquired fitting parameters into the above mobility terms, the temperature dependence of mobility for the ZnO film under the five scattering channels is shown in figure 5. One can see that ionized-impurity scattering is the dominant factor determining the mobility of the film at low temperature (<295 K in our case), while polar optical phonon scattering prevails at high temperature (>295 K in our case). In fact, ionized-impurity scattering dominates the mobility at low temperature in many semiconductors, while at elevated temperature, plenty of optical phonons exist in polar semiconductors, such as ZnO; hence, the polar optical photon scattering dominantes the mobility.

4. Conclusion

In summary, the effect of the degenerate layer at the ZnO/sapphire interface on the residual electron concentration and mobility of ZnO film has been studied. By using a two-layer conduction model, the corrected bulk electron concentration and mobility can be extracted from the Hall measurement. A fitting to the corrected electron concentration gives an activation energy E_D of 31 meV for the residual donors in ZnO. The results reported in this paper are of help in understanding the effect of the substrate on the electrical properties of ZnO films, and one can deduce from the results that by adopting substrates having smaller lattice and thermal mismatch with ZnO, the degenerate layer can be partly or totally avoided, and that high-quality ZnO films with lower residual electron concentration and higher mobility are attainable.

Acknowledgments

This work is supported by the Key Project of the National Natural Science Foundation of China under Grant No 50532050, the '973' program under Grant Nos 2006CB604906 and 2008CB317105 and the National Natural Science Foundation of China under Grant Nos 10674133, 10774132 and 60776011.

References

[1] Bhattacharya P, Das R R and Katiyar R S 2003 *Appl. Phys. Lett.* **83** 2010
[2] Tang Z K, Wong G K L, Yu P, Kawasaki M, Ohtomo A, Koinuma H and Segawa Y 1998 *Appl. Phys. Lett.* **72** 3270
[3] Tampo H, Yamada A, Fons P, Shibata H, Matsubara K, Iwata K, Niki S, Nakahara K and Takasu H 2004 *Appl. Phys. Lett.* **84** 4412
[4] Look D C and Molnar R J 1997 *Appl. Phys. Lett.* **70** 3377
[5] Götz W, Romano L T, Walker J, Johnson N M and Molnar R J 1998 *Appl. Phys. Lett.* **72** 1214
[6] Xu X L *et al* 2000 *Appl. Phys. Lett.* **76** 152
[7] Roro K T, Kassier G H, Dangbegnon J K, Sivaraya S, Westraadt J E, Neethling J H, Leitch A W R and Botha J R 2008 *Semicond. Sci. Technol.* **23** 055021
[8] Götz W, Walker J, Romano L T, Johnson N M and Molnar R J 1997 *Mater. Res. Soc. Symp. Proc.* **449** 525
[9] Lu H, Schaff W J, Eastman L F and Stutz C E 2003 *Appl. Phys. Lett.* **82** 1736
[10] Cimalla V *et al* 2003 *Phys. Status Solidi* c **0** 2818
[11] Look D C 1989 *Electrical Characterization of GaAs Materials and Devices* (New York: Wiley) chapter 1 p 117
[12] Look D C, Hemsky J W and Sizelove J R 1999 *Phys. Rev. Lett.* **82** 2552
[13] Hofmann D M, Hofstaetter A, Leiter F, Zhou H, Henecker F, Meyer B K, Orlinskii S B, Schmidt J and Baranov P G 2002 *Phys. Rev. Lett.* **88** 045504
[14] Look D C, Jones R L, Sizelove J R, Garces N Y, Giles N C and Halliburton L E 2003 *Phys. Status Solidi* a **195** 171
[15] Strzhemechny Y M, Nemergut J, Smith P E, Bae J, Look D C and Brillson L J 2003 *J. Appl. Phys.* **94** 4256
[16] Seager C H and Myers S M 2003 *J. Appl. Phys.* **94** 2888
[17] Look D C 2005 *Semicond. Sci. Technol.* **20** S55
[18] Rode D L 1975 *Semiconductors and Semimetals* vol 10 (London: Academic)
[19] Özgür Ü, Alivov Ya I, Liu C, Teke A, Reshchikov M A, Doğan S, Avrutin V, Cho S J and Morkoç H 2005 *J. Appl. Phys.* **98** 041301
[20] Orton J W and Powell M J 1980 *Rep. Prog. Phys.* **43** 1263
[21] Roth A P and Williams D F 1981 *J. Appl. Phys.* **52** 6685
[22] Qian Y H and Xu Z Z *Semiconductor Physics* (Beijing: Higher Education Press) chapter 3, pp 131–2
[23] Kohler M 1948 *Z. Phys.* **124** 772
[24] Howarthand D and Sondheimer E 1955 *Proc. R. Soc.* A **219** 53
[25] Petritz R L and Scanlon W W 1955 *Phys. Rev.* **97** 1620
[26] von Wenckstern H, Brandt M, Zimmermann G, Lenzner J, Hochmuth H, Lorenz M and Grundmann M 2007 *Mater. Res. Soc. Symp. Proc.* **957** 0957-K03-02